Nonlinear Compensation of Solar Array Simulators with Dual Power Regulation

E A Mizrah, S B Tkachev, D N Poymanov, A S Fedchenko
Reshetnev Siberian State Aerospace University
31, Krasnoyarskiy rabochiy ave., Krasnoyarsk, 660037, Russia

E-mail: alek.fedchenko@gmail.com

Abstract. During the tests of the spacecraft electrical systems there is a need for simulators of individual parts of the spacecrafts, in particular, solar array simulators (SAS). One of the topologies of medium and high power SAS simulators has dual control of consumed power and contains series or parallel connected linear and switching regulators. This topology allows to provide wide bandwidth and high efficiency, but the range of the resistance change of periodically switched SAS load is limited to the value of the stabilized attribute. Nonlinear compensator (NC) allows to reduce the average feedback voltage of the switching regulator in case of periodic load switching, which, in turn, allows to increase the average value of the stabilized attribute. The describing function method provides a mathematical description of the NC electrical circuit, which allows to select parameters of NC that eliminate the excitation of self-oscillation based on the SAS load switching frequency range and to study the switching regulator stability.

1. Introduction

Validation of electrical systems characteristics of models and experimental prototypes of the spacecraft's requires performing the special electrical tests. During these tests, as power supply sources is used devices that reproduce (with a specified error) the desired static and dynamic characteristics of the real primary power sources, in particular, solar arrays. Such devices are calling solar array simulators (SAS) [1-5]

The quality of ground-based tests is determined by the properties of used simulators, namely:

- accuracy of reproduction of static (current-voltage characteristic) and dynamic (internal impedance) characteristics of the actual solar array;
- performance properties of simulator, such as the possibility of uninterrupted operation and the possibility of durable operation in maximum loading conditions.

The most promising topology of medium and high power SAS at the moment is topology with dual control of consumed power which contains series or parallel connected linear and switching regulators [6].

A linear regulator (LR) in the SAS may be connected in series (Fig. 1a) or in parallel (Fig. 1b) with the load. The LR provides the desired characteristics of a real solar cell (current-voltage characteristics and impedance) and a switching regulator (SR) limits the power that dissipate the LR by stabilizing the LR voltage (series connection) or by stabilizing the LR current (parallel connection).

Content from this work may be used under the terms of the Creative Commons Attribution 3.0 licence. Any further distribution of this work must maintain attribution to the author(s) and the title of the work, journal citation and DOI.
Published under licence by IOP Publishing Ltd

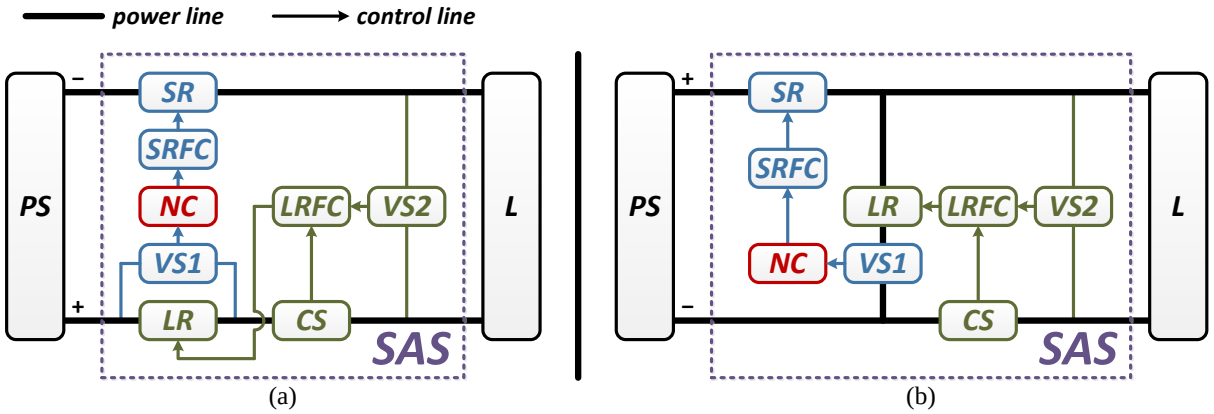

Figure 1. Block diagram of the SAS with dual control of consumed power: (a) series connection, (b) parallel connection. PS – power supply, SR – switching regulator, SRFC – switching regulator feedback circuit, NC – nonlinear compensator, LR – linear regulator, LRFC – linear regulator feedback circuit, VS – voltage sensor, CS – current sensor, L – load.

This topology combines the advantages of simulators containing only one regulator. Simulators based on individual linear regulator allow to achieve high performance rates and to ensure the accuracy of desired dynamic characteristics. Simulators based on individual switching regulator allow to achieve high values of efficiency and good weight/size ratio.

However, simulators with dual power control has problems with a broadband load switching. Since performance of the SR is considerably slower than performance of the LR, during the process of load switching from open-curcuit mode to short-curcuit mode there is a possibility that the LR will stop operate in the active region, which will lead to deterioration of the quality of electricity at a load.

In [7] was proposed the method of improving the quality of SAS operation by introducing a nonlinear compensator (NC) in the SR feedback loop. The NC belongs to the class of dynamic compensators, since the effect of its introducing becomes significant only during transients. During steady state (constant load resistance) stabilized LR attribute remains unchanged.

The purpose of the NC introduction in the feedback loop of SR - reducing the average SR feedback voltage in the case of a periodic load switching, which, in turn, will lead to an increase in value of the stabilized attribute:

- voltage across the LR – in series type simulators;
- current through the LR – in parallel type simulators.

Increasing the value of the stabilized attribute allows the LR to remain in active mode for a wider range of periodically switched resistance of SAS.

The NC may be made as a RC-circuit whose resistance R is shunted by diode VD (figure 2).

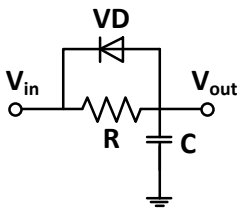

Figure 2. Circuit diagram of the nonlinear compensator.

A capacitor C charges with time constant $T_c = RC$ and discharges through a diode VD with time constant $T_d = R_e C$, where $R_e = \frac{RR_{VD}}{R + R_{VD}}$, R_{VD} – differential resistance of open diode.

In this circuit $R_{VD} \square R$, so the discharge time constant T_d is much smaller than the capacitor charge time constant T_c.Consequently, the average voltage across the capacitor decreases with a periodic load switching, which increases the average value of the LR stabilized attribute and increase switching load range, wherein the LR remains is in active mode. Thus, the introduction of the NC improves performance properties of SAS.

2. Mathematical description of solar array simulator with the nonlinear compensator

One of the common methods for the study of nonlinear systems is the describing function method [8-10]. This method allows to study the stability of the nonlinear system described by differential equations of any order.

The nonlinear system represented as a feedback connected linear part of whole nonlinear system and a nonlinearity. Assume that the signal at the input of a nonlinear system $v_{in}(\varphi)$ is sinusoidal with constant component V_0:

$$\phi_k(\vec{r}) = (2\pi)^{2/3} \exp\left(\mathrm{i}\vec{k} \cdot \vec{r}\right), \tag{1}$$

where $\varphi = \omega \cdot t$ – phase angle, ω – frequency, t – time, A – the amplitude of the harmonic component of the input voltage.

Without the diode VD, output $V_{oRC}(s)$ related to input $V_{in}(s)$ voltage of the NC as the first-order transfer function of with a time constant $T_c = RC$:

$$G_{NC}(s) = \frac{V_{oRC}(s)}{V_{in}(s)} = \frac{1}{T_c s + 1}. \tag{2}$$

The transfer function (2) corresponds to the absolute value $|G_{NC}(jd)| = R(d)$, and the argument $G_{NC}(d) = \varphi_0(d)$:

$$R(d) = |G_{NC}(jd)| = \frac{1}{\sqrt{1 + d^2}}, \tag{3}$$

$$\varphi_0(d) = \arg G(d) = -\tan^{-1}(d), \tag{4}$$

where $d = \omega \cdot T_c$ – normalized frequency.

Consider the mathematical description of the NC under asymmetric fluctuations of the input voltage $V_{in}(\varphi)$, assuming that diode is an ideal switch. The input voltage source has the following parameters: $A = 8V$, $U_0 = 20V$. The input voltage V_{in}, the output voltage of the nonlinear compensator V_{out} and the output voltage of RC circuit V_{oRC} are shown in figure 3.

The figure shows that:

- the output voltage of the NC - non-sinusoidal periodic function with period of 2π;
- voltage v_{out} in the intervals $0 < \varphi < \frac{\pi}{2}$ and $2\pi - \varphi_1 < \varphi < 2\pi$ is describing by input signal expression (1), where $\varphi_1(d)$ – angle of switching.

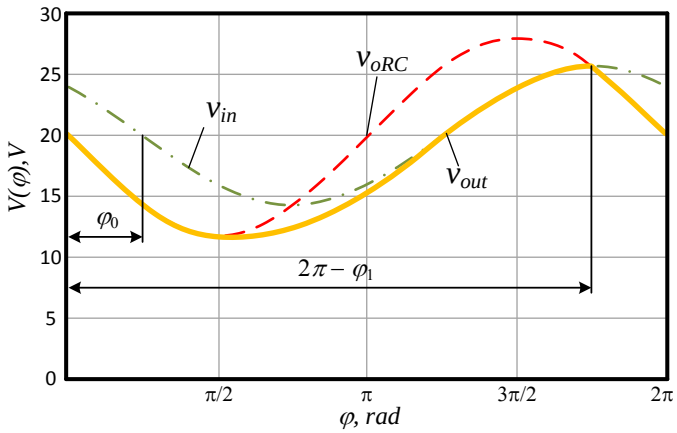

Figure 3. The nonlinear compensator voltages.

An analytical expression that describes the output voltage $v_{out}(\varphi)$ in the interval $\frac{\pi}{2} < \varphi < 2\pi - \varphi_1$ can be found from the differential equation of the NC for nonzero initial conditions and input voltage (1):

$$V_{out}(\varphi) = \begin{cases} V_0 - A\cdot\sin(\varphi), & if\ 2\pi n \le \varphi \le \dfrac{\pi}{2} + 2\pi n \\ V_0 - A\cdot R(d)\cdot\sin(\varphi-\varphi_0) - A\cdot(1-R(d)\cdot\cos(\varphi_0))\cdot e^{-\frac{\varphi-\left(\frac{\pi}{2}+2\pi n\right)}{d}} & \\ \qquad\qquad if\ \dfrac{\pi}{2} + 2\pi n \le \varphi \le 2\pi(n+1) - \varphi_1 & \\ V_0 - A\cdot\sin(\varphi), & if\ 2\pi(n+1) - \varphi_1 \le \varphi \le 2\pi(n+1) \end{cases} . \quad (5)$$

Switching angle φ_1 (figure 4) can be found numerically from the equation:

$$\frac{\sin(\varphi_1) + e^{-\frac{\frac{3\pi}{2}-\varphi_1}{d}}}{\cos(\varphi_1)} = \frac{R(d)\cdot\sin(\varphi_0)}{1-R(d)\cdot\cos(\varphi_0)} . \quad (6)$$

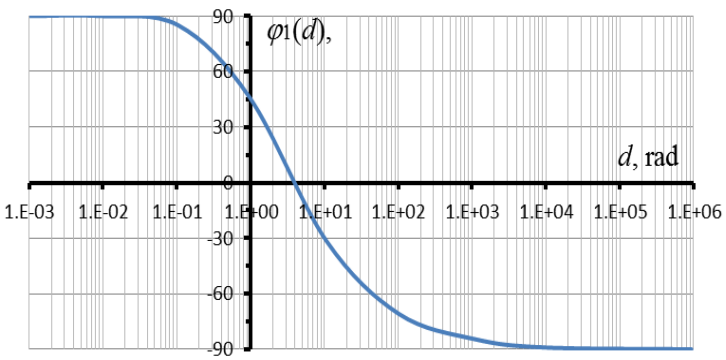

Figure 4. Normalized phase response of $\varphi_1(d)$.

Constant term of the output voltage $V_0^*(V_0, A, d)$ and describing function $H(V_0, A, d)$ of the NC can be found according to the describing function method:

$$V_0^*(V_0, A, d) = \frac{1}{\pi A}\int_0^{2\pi} V_{out}(\varphi)\, d\varphi, \tag{7}$$

$$\mathrm{Re}\, H(V_0, A, d) = \frac{1}{\pi A}\int_0^{2\pi} V_{out}(\varphi)\cdot \sin(\varphi) d\varphi, \tag{8}$$

$$\mathrm{Im}\, H(V_0, A, d) = \frac{1}{\pi A}\int_0^{2\pi} V_{out}(\varphi)\cdot \cos(\varphi) d\varphi, \tag{9}$$

From the expressions (5) and (7-9) can be found expression for constant term of output voltage $V_0^*(A, \omega, V_0)$ (10) and for the describing functions $H(A, \omega, V_0)$ (real (11) and imaginary (12) parts) in closed form:

$$\begin{aligned} V_0^*(V_0, A, d) = V_0 &- \frac{A\cdot R(d)}{2\pi}\sin(\varphi_0) - \frac{A}{2\pi}\cos(\varphi_1) - \frac{A\cdot R(d)}{2\pi}\cos(\varphi_0 - \varphi_1) \\ &+ \frac{A\cdot d}{2\pi}\cdot(1 - R(d)\cos(\varphi_0))\cdot\left(e^{-\frac{\frac{3\pi}{2}-\varphi_1}{d}} - 1\right) \end{aligned}, \tag{10}$$

$$\begin{aligned} \mathrm{Re}\, H(V_0, A, d) = &-\frac{1}{4} - \frac{1}{2\pi}\varphi_1 - \frac{R(d)}{2\pi}\cos(\varphi_0)\left(\frac{3\pi}{2} - \varphi_1\right) - \frac{R(d)}{4\pi}\sin(\varphi_0 + 2\varphi_1) \\ &- \frac{R(d)}{4\pi}\sin(\varphi_0) + \frac{1}{4\pi}\sin(2\varphi_1) - \frac{R^2(d)d}{\pi}(1 - R(d)\cos(\varphi_0)) \\ &+ \frac{R^2(d)d^2}{\pi}(1 - R(d)\cos(\varphi_0))\left(\cos(\varphi_1) - \frac{1}{d}\sin(\varphi_1)\right)\cdot e^{-\frac{\frac{3\pi}{2}-\varphi_1}{d}} \end{aligned}, \tag{11}$$

$$\begin{aligned} \mathrm{Im}\, H(V_0, A, d) = &-\frac{1}{4\pi} + \frac{R(d)}{2\pi}\sin(\varphi_0)\left(\frac{3\pi}{2} - \varphi_1\right) + \frac{R(d)}{4\pi}\cos(\varphi_0 + 2\varphi_1) \\ &+ \frac{R(d)}{4\pi}\sin(\varphi_0) - \frac{1}{4\pi}\sin(2\varphi_1) + \frac{R^2(d)d^2}{\pi}(1 - R(d)\cos(\varphi_0)) \\ &+ \frac{R^2(d)d^2}{\pi}(1 - R(d)\cos(\varphi_0))\left(\sin(\varphi_1) + \frac{1}{d}\cos(\varphi_1)\right)\cdot e^{-\frac{\frac{3\pi}{2}-\varphi_1}{d}} \end{aligned}. \tag{12}$$

The expression (10) shows that the constant component V_0^* depends on the constant component V_0, input signal amplitude A and the normalized frequency d. The expressions (11) and (12) show that the describing function H are independent of V_0 and depend only on the variable d ,that is, the charge time constant T_c and frequency ω, therefore denote it $H(d)$.

To find the parameters of the NC circuit (figure 2), the value of the normalized frequency must be determined $d = \omega T_c$. The normalized frequency d is determined as follows:

- assign the following parameters on the assumption of the required power dissipation of the LR and the maximum value of the amplitude fluctuations of the stabilized

attribute: constant input voltage V_0, input signal amplitude A and voltage reduction ratio $k_{VR} = \frac{V_R}{V_0}$, where V_R – the desired voltage drop across the switching regulator;

- plot the output voltage $V_0^*(A,d)$ by the expression (10);
- find the value of the normalized frequency d based on the value of the reduced voltage V_R and the amplitude A.

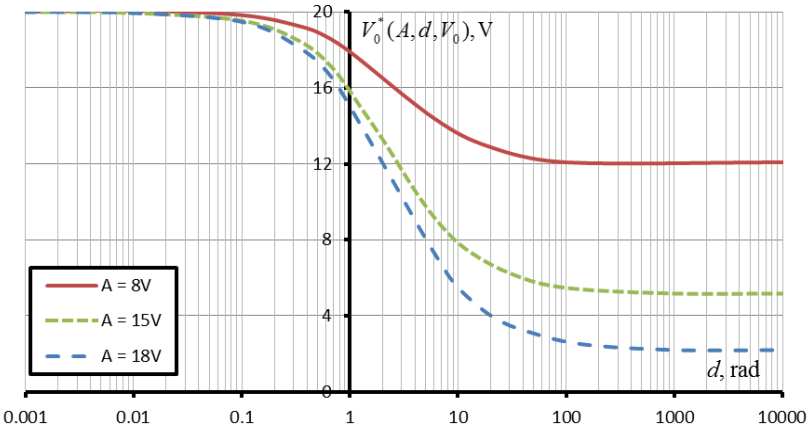

Figure 5. Constant term of the input signal at $V_0 = 20\text{V}$.

For example, for $V_R = 5.2\text{V}$ and $A = 15\text{V}$ from figure 5 can be obtained $d = 100\text{rad}$. Then, assigning the load switching frequency, the time constant can be found as $T_c \approx \frac{d}{\omega} = RC$. Parameters R and C of the NC are selected taking into account the impedance matching of the input circuits of subsequent devices.

After finding the time constant T_c it necessary to check the stability of the SR control system for self-oscillations. Since the bandwidth of the SR is much smaller than the pulse modulation frequency, on the basis of Nyquist-Shannon sampling theorem we will consider the SR as a continuous system.

According to the describing function method [8] characteristic equation is written as negative reciprocal of a linear system transfer function $G(j\omega)$:

$$G(j\omega) = -\frac{1}{H(d)}, \tag{13}$$

For example, we use the following form of the SR linear system transfer function consisting of a second-order filter and compensator:

$$G(j\omega) = \frac{(T_2 s + 1)}{(T_1 s + 1)} \cdot \frac{K}{\left(T_3^2 s^2 + 2\xi T_3 s + 1\right)}, \tag{14}$$

where $T_1 = 0.34\text{s}$, $T_2 = 7.88 \cdot 10^{-5}\text{s}$, $T_2 = 7.74 \cdot 10^{-5}\text{s}$, $\xi = 0.133$, $K = 220$.

Since the curves of $G(j\omega)$ and $-\frac{1}{H(d)}$ (figure 6) do not overlap, there is no real value of the oscillation frequency, and, therefore, no self-oscillation. However, with the increase of the SR bandwidth due to changes in the parameters of $G(j\omega)$, it is possible that loci can intersect and self-oscillation will occur.

3. Simulation results

For the topology of SAS with the LR voltage stabilization (figure 1 (a)), using circuit simulation package Micro-cap, the transients of SAS without the NC (figure 6) and with the NC (figure 7) were plotted for the following conditions: a load resistance R_L changed rapidly from 0.1 Ohm to 1 Ohm (current region of current-voltage characteristics), the LR stabilized voltage $v_{LR} = 10\text{V}$.

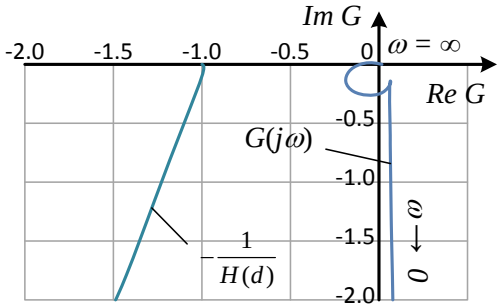

Figure 6. Constant term of the input signal at $V_0 = 20\text{V}$.

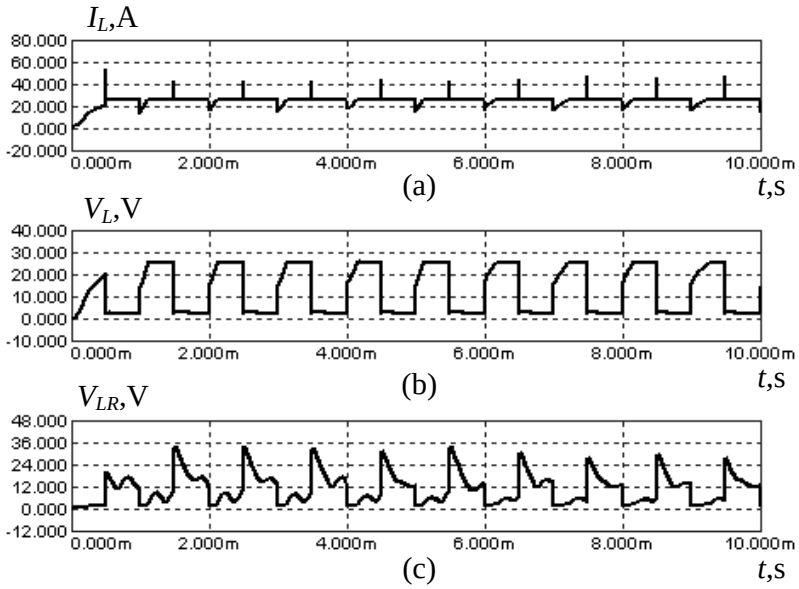

Figure 7. Load switching response without the NC (RL1 = 0.1 Ohm, RL2 = 1 Ohm, VLR = 10 V): (a) load current, (b) load voltage, (c) output voltage of linear regulator.

The figures 7 and 8 show that during the load reducing (decreasing of load current i_L and increasing of load voltage v_L) the LR voltage v_{LR} is reduced almost to zero. This is due to the fact that the switching regulator has a considerably greater inertia than the linear regulator, it does not have time to stabilize the voltage drop during the stepped load resistance switching. Therefore, when the voltage pulse amplitude of the load exceeds the value of the stabilized voltage to the LR, a further increase in the voltage v_L is determined by a switching regulator, and the shape of the voltage v_L is significantly different from the desired square.

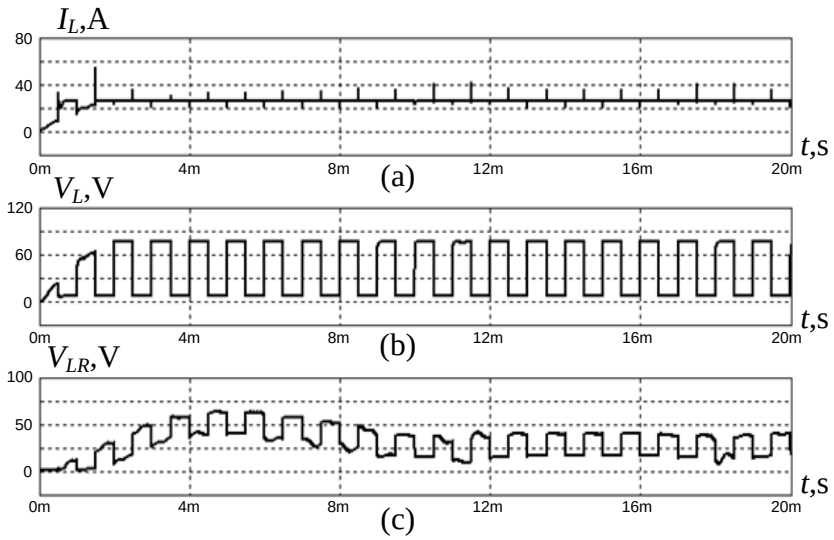

Figure 8. Load switching response with the NC (RL1 = 0.1 Ohm, RL2 = 1 Ohm, VLR = 10 V): (a) load current, (b) load voltage, (c) output voltage of linear regulator.

The figures show that the introduction of the NC is quite effective: in the same load resistance switching range a minimum voltage at the LR is greater than zero, so the LR operates in active mode, and the load voltage v_L has the required form.

4. Conclusion

The paper studied the impact of parameters of the nonlinear compensator (NC) on the stability of medium and high power solar array simulator (SAS) control system by the describing function method. The parameters of the NC, which preclude the self-oscillations, were defined. The following results were obtained:

- the introduction of the NC in the feedback loop of the switching regulator allows to extend the range of the periodically switched resistance of the SAS;
- using the describing function method a mathematical description of the proposed NC circuit was developed, this description allows to select the parameters of NC based on load switching frequency range of the SAS;
- the describing functions of the NC allow to explore the impact of the dynamic properties of the NC on the switching regulator stability.

The simulation shows that the introduction of the NC is quite effective: in the same load resistance switching range a minimum voltage at the LR is greater than zero, so the LR operates in active mode, and the load voltage has the required form.

Acknowledgements

This study was supported by the Ministry of Education and Science of the Russian Federation (Government Contract 14.577.21.0082, unique identifier RFMEFI57714X0082).

References

[1] Lloyd S H, Smith G A, Infield D G 2000 Design and construction of a modular electronic photovoltaic simulator *Proc. of the 8th Intern. Conf. on Power Electronics and Variable Speed Drives* (London, UK) pp 120–123

[2] Rahmani N, Mostefai M 2013 Experimental results of a photovoltaic simulator

Conference Internationale des Energies Renouvelables (CIER'13) (Sousse, Tunisie) volume **2**
[3] Agilent E4350B, E4351B Modular Solar Array Simulators Datasheet www.agilent.com
[4] Elgar Solar Array Simulators. www.elgar.com
[5] Utility model # 144248 Russian Federation. Elektricheskiy imitator solnechnoj batarei (Electrical solar array simulator) / V.N. Mishin, V.A. Pchelnikov, O.V. Bubnov, Ju.A. Kremzukov – 20.08.2014. Tomsk state university of control systems and radioelectronics
[6] Tkachev S B, Mizrah E A 2011 Upgrading of photovoltaic array simulator with two-circuit control element *Vestnik SibGAU* **1 (34)** pp 70–75
[7] Mizrah E A, Tkachev S B, Shtabel N V and Poymanov D N 2015 Design Principles Of Space Power System Primary Energy Sources Simulators *International Journal of Applied Engineering Research* (vol. **10**) (Dehli: Research India Publications) number 20 pp 41136–41142
[8] Lurie B J, Enright P J 2012 *Classical Feedback Control: With MATLAB and Simulink, Second Edition* (FL: CRC Press) p 556
[9] Mizrah E.A., Sidorov A.S. Modeling of solar array simulator with cascade connection of continuous and impulse power amplifier *Vestnik SibGAU* **1 (14)** pp 7–12
[10] Impram S T, Munro Neil 2010 Describing functions in non-linear systems with structured and unstructured uncertainties *International Journal of Control* (vol.**74**) (Taylor and Francis) issue 6 pp 600–608